

Observations of Low and Intermediate Spectral Peak Blazars with the Imaging X-ray Polarimetry Explorer

HERMAN L. MARSHALL,¹ IOANNIS LIODAKIS,² ALAN P. MARSCHER,³ NICCOLÒ DI LALLA,⁴ SVETLANA G. JORSTAD,^{3,5}
DAWOON E. KIM,^{6,7,8} RICCARDO MIDDEI,^{9,10} MICHELA NEGRO,^{11,12,13} NICOLA OMODEI,⁴ ABEL L. PEIRSON,⁴
MATTEO PERRI,^{9,14} SIMONETTA PUC CETTI,⁹ IVÁN AGUDO,¹⁵ GIACOMO BONNOLI,^{16,15} ANDREI V. BERDYUGIN,¹⁷
ELISABETTA CAVAZZUTI,¹⁸ NICOLE RODRIGUEZ CAVERO,¹⁹ IMMACOLATA DONNARUMMA,¹⁸ LAURA DI GESU,¹⁸
JENNI JORMANAINEN,^{2,17} HENRIC KRAWCZYNSKI,¹⁹ ELINA LINDFORS,² FRÉDÉRIC MARIN,²⁰ FRANCESCO MASSARO,^{21,22}
LUIGI PACCIANI,⁶ JURI POUTANEN,^{23,24} FABRIZIO TAVECCHIO,²⁵ POUYA M. KOUCH,^{2,26} FRANCISCO JOSÉ ACEITUNO,¹⁵
MARIA I. BERNARDOS,¹⁵ GIACOMO BONNOLI,^{25,15} VÍCTOR CASANOVA,¹⁵ MAYA GARCÍA-COMAS,¹⁵
BEATRIZ AGÍS-GONZÁLEZ,¹⁵ CÉSAR HUSILLOS,¹⁵ ALESSANDRO MARCHINI,²⁷ ALFREDO SOTA,¹⁵ DMITRY BLINOV,^{28,29,30}
IOAKE G. BOURBAH,³⁰ SEBASTIAN KIELHMANN,^{28,30} EVANGELOS KONTOPODIS,³⁰ NIKOS MANDARAKAS,^{28,30}
STYLIANOS ROMANOPOULOS,^{29,30} RAPHAEL SKALIDIS,^{28,30} ANNA VERVELAKI,³⁰ GEORGE A. BORMAN,³¹
EVGENIA N. KOPATSKAYA,⁵ ELENA G. LARIONOVA,⁵ DARIA A. MOROZOVA,⁵ SERGEY S. SAVCHENKO,^{5,32,33}
ANDREY A. VASILYEV,⁵ ALEXEY V. ZHOVTAN,³¹ CAROLINA CASADIO,^{28,30} JUAN ESCUDERO,³⁴ JOANA KRAMER,³⁵
IOANNIS MYSERLIS,³⁶ EFTHALIA TRAINOU,³⁷ RYO IMAZAWA,³⁸ MAHITO SASADA,³⁹ YASUSHI FUKAZAWA,^{38,40,41}
KOJI S. KAWABATA,^{38,40,41} MAKOTO UEMURA,^{38,40,41} TSUNEFUMI MIZUNO,⁴⁰ TATSUYA NAKAOKA,⁴⁰ HIROSHI AKITAYA,⁴²
JOSEPH R. MASIERO,⁴³ DIMITRI MAWET,⁴³ MAXWELL A. MILLAR-BLANCHAER,⁴⁴ GEORGIA V. PANOPOULOU,⁴³
SAMAPORN TINYANONT,⁴⁵ MASATO KAGITANI,⁴⁶ VADIM KRAVTSOV,¹⁷ TAKESHI SAKANOI,⁴⁶ LUCIO A. ANTONELLI,^{14,9}
MATTEO BACHETTI,⁴⁷ LUCA BALDINI,^{48,49} WAYNE H. BAUMGARTNER,⁵⁰ RONALDO BELLAZZINI,⁴⁸ STEFANO BIANCHI,⁵¹
STEPHEN D. BONGIORNO,⁵⁰ RAFFAELLA BONINO,^{21,52} ALESSANDRO BREZ,⁴⁸ NICCOLÒ BUCCIANINI,^{53,54,55}
FIAMMA CAPITANIO,⁶ SIMONE CASTELLANO,⁴⁸ CHEN-TING CHEN,⁵⁶ STEFANO CIPRINI,^{57,9} ENRICO COSTA,⁶
ALESSANDRA DE ROSA,⁶ ETTORE DEL MONTE,⁶ ALESSANDRO DI MARCO,⁶ VICTOR DOROSHENKO,⁵⁸ MICHAL DOVČIAK,⁵⁹
STEVEN R. EHLERT,⁵⁰ TERUAKI ENOTO,⁶⁰ YURI EVANGELISTA,⁶ SERGIO FABIANI,⁶ RICCARDO FERRAZZOLI,⁶
JAVIER A. GARCIA,^{43,12} SHUICHI GUNJI,⁶¹ KIYOSHI HAYASHIDA,⁶² JEREMY HEYL,⁶³ WATARU IWAKIRI,⁶⁴ PHILIP KAARET,⁵⁰
VLADIMIR KARAS,⁵⁹ FABIAN KISLAT,⁶⁵ TAKAO KITAGUCHI,⁶⁰ JEFFERY J. KOLODZIEJCZAK,⁵⁰ FABIO LA MONACA,⁶
LUCA LATRONICO,²¹ SIMONE MALDERA,²¹ ALBERTO MANFREDI,⁴⁸ ANDREA MARINUCCI,¹⁸ GIORGIO MATT,⁵¹
IKUYUKI MITSUISHI,⁶⁶ FABIO MULERI,⁶ C.-Y. NG,⁶⁷ STEPHEN L. O'DELL,⁵⁰ CHIARA OPPEDISANO,²¹
ALESSANDRO PAPIITTO,¹⁴ GEORGE G. PAVLOV,⁶⁸ MELISSA PESCE-ROLLINS,⁴⁸ PIERRE-OLIVIER PETRUCCI,⁶⁹ MAURA PILIA,⁴⁷
ANDREA POSSENTI,^{47,24} BRIAN D. RAMSEY,⁵⁰ JOHN RANKIN,⁶ AJAY RATHEESH,⁶ OLIVER J. ROBERTS,⁵⁶
ROGER W. ROMANI,⁴ CARMELO SGRÒ,⁴⁸ PATRICK SLANE,⁷⁰ PAOLO SOFFITTA,⁶ GLORIA SPANDRE,⁴⁸ DOUGLAS A. SWARTZ,⁵⁶
TORU TAMAGAWA,⁶⁰ ROBERTO TAVERNA,⁷¹ YUZURU TAWARA,⁶⁶ ALLYN F. TENNANT,⁵⁰ NICHOLAS E. THOMAS,⁵⁰
FRANCESCO TOMBESI,^{72,57,73} ALESSIO TROIS,⁴⁷ SERGEY S. TSYGANKOV,¹⁷ ROBERTO TUROLLA,^{71,74} JACCO VINK,⁷⁵
MARTIN C. WEISSKOPF,⁵⁰ KINWAH WU,⁷⁴ FEI XIE,^{76,6} AND SILVIA ZANE⁷⁴

¹MIT Kavli Institute for Astrophysics and Space Research, Massachusetts Institute of Technology, 77 Massachusetts Avenue, Cambridge, MA 02139, USA

²Finnish Centre for Astronomy with ESO, 20014 University of Turku, Finland

³Institute for Astrophysical Research, Boston University, 725 Commonwealth Avenue, Boston, MA 02215, USA

⁴Department of Physics and Kavli Institute for Particle Astrophysics and Cosmology, Stanford University, Stanford, California 94305, USA

⁵St. Petersburg State University, St. Petersburg, 199034 Russia

⁶INAF Istituto di Astrofisica e Planetologia Spaziali, Via del Fosso del Cavaliere 100, 00133 Roma, Italy

⁷Dipartimento di Fisica, Università degli Studi di Roma "La Sapienza", Piazzale Aldo Moro 5, 00185 Roma, Italy

⁸Dipartimento di Fisica, Università degli Studi di Roma "Tor Vergata", Via della Ricerca Scientifica 1, 00133 Roma, Italy

⁹Space Science Data Center, Agenzia Spaziale Italiana, Via del Politecnico snc, 00133 Roma, Italy

¹⁰INAF Osservatorio Astronomico di Roma, Via Frascati 33, 00040 Monte Porzio Catone (RM), Italy

¹¹University of Maryland, Baltimore County, Baltimore, MD 21250, USA

¹²NASA Goddard Space Flight Center, Greenbelt, MD 20771, USA

¹³Louisiana State University, Baton Rouge, LA 70803, USA

¹⁴INAF Osservatorio Astronomico di Roma, Via Frascati 33, 00078 Monte Porzio Catone (RM), Italy

¹⁵Instituto de Astrofísica de Andalucía (CSIC), Apartado 3004, E-18080 Granada, Spain

- ¹⁶ *INAF – Osservatorio Astronomico di Brera, via E. Bianchi 46, I-23807 Merate, Italy*
- ¹⁷ *Department of Physics and Astronomy, University of Turku, FI-20014, Finland*
- ¹⁸ *Agenzia Spaziale Italiana, Via del Politecnico snc, 00133 Roma, Italy*
- ¹⁹ *Physics Department and McDonnell Center for the Space Sciences, Washington University in St. Louis, St. Louis, MO 63130, USA*
- ²⁰ *Université de Strasbourg, CNRS, Observatoire Astronomique de Strasbourg, UMR 7550, 67000 Strasbourg, France*
- ²¹ *Istituto Nazionale di Fisica Nucleare, Sezione di Torino, Via Pietro Giuria 1, 10125 Torino, Italy*
- ²² *Dipartimento di Fisica, Università degli Studi di Torino, Via Pietro Giuria 1, 10125 Torino, Italy*
- ²³ *Department of Physics and Astronomy, University of Turku, 20014 Turku, Finland*
- ²⁴ *Space Research Institute of the Russian Academy of Sciences, Profsoyuznaya Str. 84/32, Moscow 117997, Russia*
- ²⁵ *INAF Osservatorio Astronomico di Brera, Via E. Bianchi 46, 23807 Merate (LC), Italy*
- ²⁶ *Department of Physics and Astronomy, 20014 University of Turku, Finland*
- ²⁷ *University of Siena, Department of Physical Sciences, Earth and Environment, Astronomical Observatory, Via Roma 56, 53100 Siena, Italy*
- ²⁸ *Institute of Astrophysics, Foundation for Research and Technology-Hellas, GR-71110 Heraklion, Greece*
- ²⁹ *Institute of Astrophysics, Voutes, 7110, Heraklion, Greece*
- ³⁰ *Department of Physics, University of Crete, 70013, Heraklion, Greece*
- ³¹ *Crimean Astrophysical Observatory RAS, P/O Nauchny, 298409, Crimea*
- ³² *Special Astrophysical Observatory, Russian Academy of Sciences, 369167, Nizhnii Arkhyz, Russia*
- ³³ *Pulkovo Observatory, St. Petersburg, 196140, Russia*
- ³⁴ *Instituto de Astrofísica de Andalucía-CSIC, Glorieta de la Astronomía s/n, 18008, Granada, Spain*
- ³⁵ *Max Planck Institute for Radio Astronomy, Auf dem Huegel 69, Bonn, Germany*
- ³⁶ *Institut de Radioastronomie Millimétrique, Avenida Divina Pastora, 7, Local 20, E-18012 Granada, Spain*
- ³⁷ *Instituto de Astrofísica de Andalucía, IAA-CSIC, Glorieta de la Astronomía s/n, 18008 Granada, Spain*
- ³⁸ *Department of Physics, Graduate School of Advanced Science and Engineering, Hiroshima University Kagamiyama, 1-3-1 Higashi-Hiroshima, Hiroshima 739-8526, Japan*
- ³⁹ *Department of Physics, Tokyo Institute of Technology, 2-12-1 Ookayama, Meguro-ku, Tokyo 152-8551, Japan*
- ⁴⁰ *Hiroshima Astrophysical Science Center, Hiroshima University 1-3-1 Kagamiyama, Higashi-Hiroshima, Hiroshima 739-8526, Japan*
- ⁴¹ *Core Research for Energetic Universe (Core-U), Hiroshima University, 1-3-1 Kagamiyama, Higashi-Hiroshima, Hiroshima 739-8526, Japan*
- ⁴² *Planetary Exploration Research Center, Chiba Institute of Technology 2-17-1 Tsudanuma, Narashino, Chiba 275-0016, Japan*
- ⁴³ *California Institute of Technology, 1200 E. California Blvd., Pasadena, CA, 91125, USA*
- ⁴⁴ *University of California, Santa Barbara, CA 93106, USA*
- ⁴⁵ *University of California Santa Cruz, 1156 High Street, Santa Cruz, CA 95064 USA*
- ⁴⁶ *Graduate School of Sciences, Tohoku University, Aoba-ku, 980-8578 Sendai, Japan*
- ⁴⁷ *INAF Osservatorio Astronomico di Cagliari, Via della Scienza 5, 09047 Selargius (CA), Italy*
- ⁴⁸ *Istituto Nazionale di Fisica Nucleare, Sezione di Pisa, Largo B. Pontecorvo 3, 56127 Pisa, Italy*
- ⁴⁹ *Dipartimento di Fisica, Università di Pisa, Largo B. Pontecorvo 3, 56127 Pisa, Italy*
- ⁵⁰ *NASA Marshall Space Flight Center, Huntsville, AL 35812, USA*
- ⁵¹ *Dipartimento di Matematica e Fisica, Università degli Studi Roma Tre, Via della Vasca Navale 84, 00146 Roma, Italy*
- ⁵² *Dipartimento di Fisica, Università degli Studi di Torino, Via Pietro Giuria 1, 10125 Torino, Italy*
- ⁵³ *INAF Osservatorio Astrofisico di Arcetri, Largo Enrico Fermi 5, 50125 Firenze, Italy*
- ⁵⁴ *Dipartimento di Fisica e Astronomia, Università degli Studi di Firenze, Via Sansone 1, 50019 Sesto Fiorentino (FI), Italy*
- ⁵⁵ *Istituto Nazionale di Fisica Nucleare, Sezione di Firenze, Via Sansone 1, 50019 Sesto Fiorentino (FI), Italy*
- ⁵⁶ *Space and Technology Institute, Universities Space Research Association, Huntsville, AL 35805, USA*
- ⁵⁷ *Istituto Nazionale di Fisica Nucleare, Sezione di Roma “Tor Vergata”, Via della Ricerca Scientifica 1, 00133 Roma, Italy*
- ⁵⁸ *Institut für Astronomie und Astrophysik, Universität Tübingen, Sand 1, 72076 Tübingen, Germany*
- ⁵⁹ *Astronomical Institute of the Czech Academy of Sciences, Boční II 1401/1, 14100 Praha 4, Czech Republic*
- ⁶⁰ *RIKEN Cluster for Pioneering Research, 2-1 Hirosawa, Wako, Saitama 351-0198, Japan*
- ⁶¹ *Yamagata University, 1-4-12 Kojirakawa-machi, Yamagata-shi 990-8560, Japan*
- ⁶² *Osaka University, 1-1 Yamadaoka, Suita, Osaka 565-0871, Japan*
- ⁶³ *University of British Columbia, Vancouver, BC V6T 1Z4, Canada*
- ⁶⁴ *International Center for Hadron Astrophysics, Chiba University, Chiba, 263-8522, Japan*
- ⁶⁵ *Department of Physics and Astronomy and Space Science Center, University of New Hampshire, Durham, NH 03824, USA*
- ⁶⁶ *Graduate School of Science, Division of Particle and Astrophysical Science, Nagoya University, Furo-cho, Chikusa-ku, Nagoya, Aichi 464-8602, Japan*
- ⁶⁷ *Department of Physics, The University of Hong Kong, Pokfulam, Hong Kong*
- ⁶⁸ *Department of Astronomy and Astrophysics, Pennsylvania State University, University Park, PA 16802, USA*

⁶⁹*Université Grenoble Alpes, CNRS, IPAG, 38000 Grenoble, France*

⁷⁰*Harvard & Smithsonian Center for Astrophysics, 60 Garden St, Cambridge, MA 02138, USA*

⁷¹*Dipartimento di Fisica e Astronomia, Università degli Studi di Padova, Via Marzolo 8, 35131 Padova, Italy*

⁷²*Dipartimento di Fisica, Università degli Studi di Roma “Tor Vergata”, Via della Ricerca Scientifica 1, 00133 Roma, Italy*

⁷³*Department of Astronomy, University of Maryland, College Park, Maryland 20742, USA*

⁷⁴*Mullard Space Science Laboratory, University College London, Holmbury St Mary, Dorking, Surrey RH5 6NT, UK*

⁷⁵*Anton Pannekoek Institute for Astronomy & GRAPPA, University of Amsterdam, Science Park 904, 1098 XH Amsterdam, The Netherlands*

⁷⁶*Guangxi Key Laboratory for Relativistic Astrophysics, School of Physical Science and Technology, Guangxi University, Nanning 530004, China*

(Received October 23, 2023)

Submitted to *Astrophysical Journal*

ABSTRACT

We present X-ray polarimetry observations from the Imaging X-ray Polarimetry Explorer (IXPE) of three low spectral peak and one intermediate spectral peak blazars, namely 3C 273, 3C 279, 3C 454.3, and S5 0716+714. For none of these objects was IXPE able to detect X-ray polarization at the 3σ level. However, we placed upper limits on the polarization degree at $\sim 10\text{--}30\%$. The undetected polarizations favor models where the X-ray band is dominated by unpolarized photons upscattered by relativistic electrons in the jets of blazars, although hadronic models are not completely eliminated. We discuss the X-ray polarization upper limits in the context of our contemporaneous multiwavelength polarization campaigns.

1. INTRODUCTION

Blazars are active galactic nuclei (AGN) with relativistic jets that are inferred to be oriented within a few degrees from the observer’s line of sight (cf. [Blandford et al. 2019](#)). Their spectral energy distributions (SEDs) are generally characterized by two emission components: one at low photon energies (radio through optical, UV, and, in some cases, X-ray bands) and the other at much higher (X-ray and γ -ray) energies. Blazars are often classified by the frequency at which the low-energy portion of the SED peaks. This component is modeled as electron synchrotron emission. When the peak frequency is below the optical or infrared (IR) band, the blazar is considered to be low-synchrotron-peaked (LSP), in contrast with high-synchrotron-peaked (HSP) blazars, whose peak is in the X-ray band. Objects with a peak in the optical/UV range are termed intermediate-synchrotron-peaked (ISP) blazars.

Several LSP/ISP blazars were observed in 2022 with the Imaging X-ray Polarimetry Explorer (IXPE, [Weisskopf et al. 2022](#)) that was launched on 2021 December 9. HSP blazars such as Mrk 501 ([Liodakis et al. 2022](#)), Mrk 421 ([Di Gesu et al. 2022b](#)), and PG 1553+113 ([Middei et al. 2023](#)) were measured by IXPE to be polarized in the 10–15% range, 2–5 times higher than the optical polarization at the same epochs. These findings support a model by which the X-rays in HSPs are produced in energy-stratified shocks, with electrons accelerated at the shock front to energies high enough to emit X-ray synchrotron radiation. Such energetic electrons occur only in a thin layer close to the shock front, beyond which the maximum electron energy decreases owing to radiative cooling ([Marscher & Gear 1985](#)). Consequently, the optically emitting region, which requires somewhat lower electron energies, extends over a more extensive volume. If the magnetic field is mostly disordered, e.g., by turbulence, then the mean polarization is expected to be stronger and more highly variable over the smaller volume from which the X-rays arise ([Di Gesu et al. 2022a](#)). The ratio of X-ray to optical polarization was observed to be higher than expected in such a model, which suggests that the level of disorder of the magnetic field increases with distance from the shock front ([Liodakis et al. 2022](#); [Marscher & Jorstad 2022](#)). The alignment of the electric vector position angle (EVPA) with the jet direction in Mrk 501 ([Liodakis et al. 2022](#)) implies that there is an ordered component to the magnetic field perpendicular to the jet. How this component arises is somewhat uncertain; various suggestions involve compression of the disordered field at the shock ([Hughes et al. 1985](#)), generation of a magnetic field component transverse to the shock normal ([Tavecchio et al. 2018](#)), or a toroidal magnetic field component in the ambient jet ([Lyutikov et al. 2005](#)). Complicating the physical picture of HSP blazar shocks are the observations that the EVPA can rotate in the X-ray band without rotation in the optical ([Di Gesu et al. 2023](#)) or vice versa ([Middei et al. 2023](#)).

On the other hand, the X-ray portions of the SEDs of LSP and ISP blazars generally have flatter spectra than at optical frequencies (e.g., [Abdo et al. 2010](#)), indicating that a single synchrotron model is not responsible for both bands. The flatter X-ray spectra are consistent with models where the X-ray band is dominated by Compton upscattering of low frequency (e.g. infrared) photons by the relativistic electrons generating the synchrotron radiation (e.g., [Maraschi et al. 2008](#)). Processes involving hadrons, such as proton synchrotron radiation or production of electron-positron pairs by particle cascades might also be involved in generating the X-rays (e.g., [Zhang et al. 2016](#)). Each of these processes has specific polarization properties that can potentially identify their level of importance in the X-ray emission (e.g., [Liodakis et al. 2019](#); [Peirson et al. 2022](#)). Compton scattering of unpolarized seed photons, such as those produced by the broad emission-line region, produces essentially unpolarized high-energy photons ([Krawczynski 2012](#)). If the seed photons are from synchrotron radiation in the jet — the synchrotron self-Compton (SSC) case — the X-ray polarization fraction (Π_X) is generally less than half that of the synchrotron radiation; the exact ratio depends on the model and the level of disorder of the magnetic field ([Peirson et al. 2022](#)). For hadronic processes, Π_X is expected to be similar or even exceed the optical polarization (Π_O) ([Zhang & Böttcher 2013](#); [Zhang et al. 2019](#)). Hence, X-ray polarization measurements or even upper limits in the context of simultaneous multiwavelength polarization observations can test emission models for LSP and ISP blazars.

IXPE previously observed BL Lac on three occasions. In the first two observations, the X-ray spectrum of BL Lac resembled that of LSPs, in the third observation that of ISPs. During the first two observations, there was only a 99% confidence upper limit of $\Pi_X < 13\%$, while the contemporaneous Π_O exceeded the X-ray limits ([Middei et al. 2023](#)). In the third observation, 22% polarization was detected in the 2–4 keV band during a time dominated by synchrotron-emitting electrons from the low-energy hump of the SED ([Peirson et al. 2023](#)). There are still only upper limits to the X-ray polarization from the high-energy component. Those results disfavor any significant contribution from protons to the emission.

In this study, we present results from IXPE observations of three LSP blazars and one ISP blazar that were observed in 2022: 3C 273, 3C 279, 3C 454.3, and S5 0716+714. In section 2 we describe the IXPE observations with full-band polarimetric and spectropolarimetric analyses, in section 3 we discuss the multiwavelength polarization campaigns on individual sources, and in section 4 we discuss our results.

2. IXPE OBSERVATIONS

A log of IXPE observations is provided in Table 1. See [Weisskopf et al. \(2022\)](#) for details about IXPE. At the $\sim 30''$ angular resolution of IXPE, all of these sources are spatially unresolved.

2.1. Full-Band Analyses

Event data were selected over the full bandpass from 2 to 8 keV, from a circular region $60''$ radius about each source, with background selected from an annulus from $200''$ to $300''$ from the target. Data were processed using `ixpeobssim` ([Baldini et al. 2022](#)) and standard `ftools` [NASA High Energy Astrophysics Science Archive Research Center \(HEASARC\) \(2014\)](#). Background-subtracted light curves are shown in Fig. 1.

Results from an unbinned event-based likelihood analysis ([Marshall 2021](#)) that accounts for an unpolarized background ([Marshall 2023](#)) are shown in Fig. 2. No clear detections of X-ray polarizations are observed at the 1–2 σ confidence level, with 99% confidence limits ranging from 9% to 28% (Table 1).

Rotations of the EVPA during the IXPE observation, especially for exposures longer than the typical variability timescales (~ 1 – 2 days) in blazars, can lead to depolarization, as was demonstrated recently in the X-ray EVPA rotation detected by IXPE in Mrk 421 ([Di Gesu et al. 2023](#)). We tested for rotations using the method described in [Di Gesu et al. \(2023\)](#), employing an event-based likelihood method ([Marshall 2021](#)). Briefly, event tracks are rotated according to a simple model where the EVPA rotates uniformly through the observation with rate ω (in degrees per day). The difference in the log-likelihood is $\Delta S = S(\omega; \hat{q}, \hat{u}) - S(0; \hat{q}_0, \hat{u}_0)$, where $S(\omega; \hat{q}, \hat{u})$ is the log likelihood at ω at the best fit q and u for that value of ω . ΔS is distributed as χ^2 with one degree of freedom because q and u are uninteresting parameters for this test. We do not find evidence for EVPA rotations during our observations in any of the four sources. An example of the results from a rotation search is shown in Fig. 3.

2.2. Spectropolarimetry

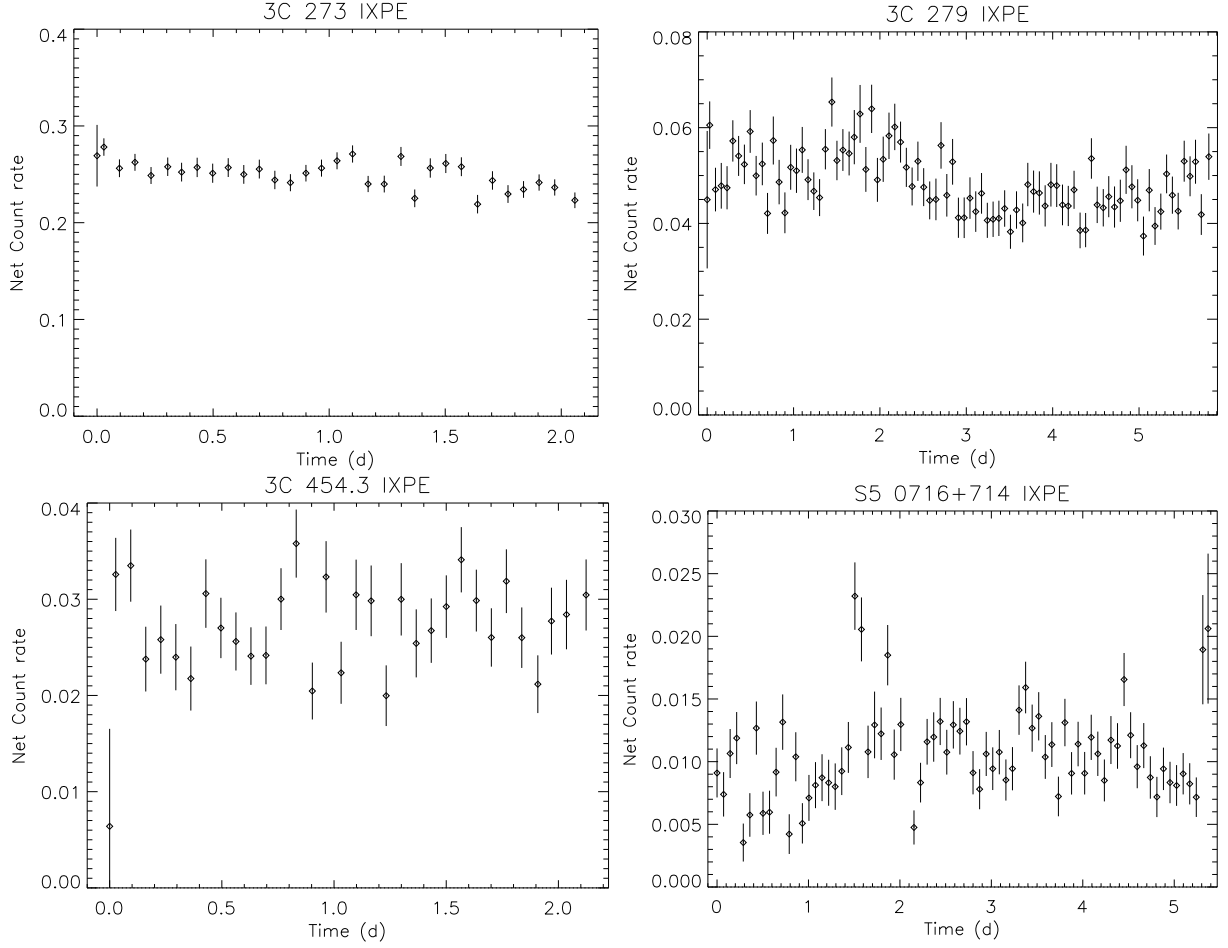


Figure 1. IXPE background-subtracted light curves for the four blazars reported here. No large variations are observed that would warrant isolating specific time periods for detailed analysis.

Table 1. Summary of IXPE Observations

Source	Instrument	Observation ID	MJD range	Exposure (ks) ^a	Π_X ^b
3C 273	IXPE	01005901	59732.37 - 59734.45	95.28	< 9.0%
3C 279	IXPE	01005701	59743.02 - 59748.85	264.42	< 12.7%
3C 454.3	IXPE	01005401	59730.19 - 59732.34	98.12	< 28%
S5 0716+714	IXPE	01005301	59669.43 - 59674.80	358.68	< 26%

^a Average of exposures for the three detector units.

^b 99% confidence limits using the unbinned, event-based likelihood method (§ 2.1).

Spectropolarimetric fits were performed with the Multi-Mission Maximum Likelihood (3ML) framework¹ (Vianello et al. 2015). In the 2–8 keV energy range, the spectra for the four sources are well described by an absorbed power law. The absorption column densities were fixed to the nominal Galactic values,² and the polarization parameters

¹ <https://threeml.readthedocs.io/en/stable/index.html>

² <https://heasarc.gsfc.nasa.gov/cgi-bin/Tools/w3nh/w3nh.pl>

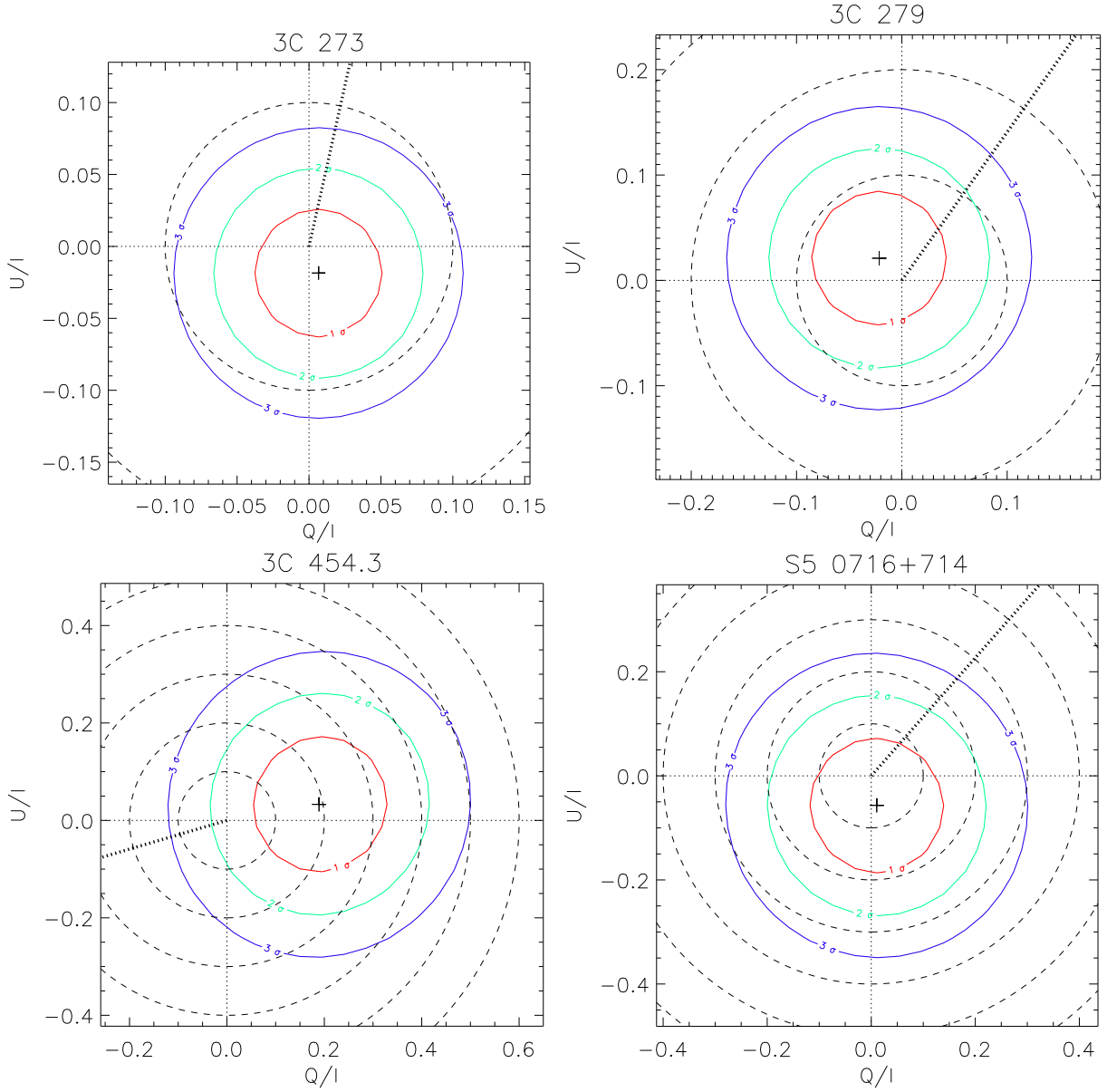


Figure 2. Probability contours in $Q - U$ space for time- and bandpass-averaged IXPE polarimetry of four blazars using a maximum likelihood method that accounts for unpolarized background. Contour levels for two degrees of freedom enclose the 1σ , 2σ , and 3σ confidence regions. The plus signs mark the best estimates of $q = Q/I$ and $u = U/I$ and the dashed lines give circles of constant X-ray polarization fraction $\Pi_X = (q^2 + u^2)^{1/2}$ in 10% increments. The PAs of the jets are indicated by the thick dotted lines, taken from . In all cases, the results are consistent with null polarization at the 1– 2σ confidence level.

are assumed to be constant through each observation and independent of energy. Table 2 summarizes the best-fit parameters from the fits to each source and Fig. 4 shows the spectral fits. Fig. 5 and Fig. 6 show the polarization parameters derived from the spectropolarimetric fits. An analysis using `xspec` gave similar results.

3. NOTES ON INDIVIDUAL SOURCES

Here we give information regarding the individual sources and our contemporaneous multiwavelength campaign during the IXPE observations. The results from the multiwavelength campaigns are summarized in Appendix A and in Figs. 7, 8, 9, and 10, and Tables 3, 4, 5, and 6.

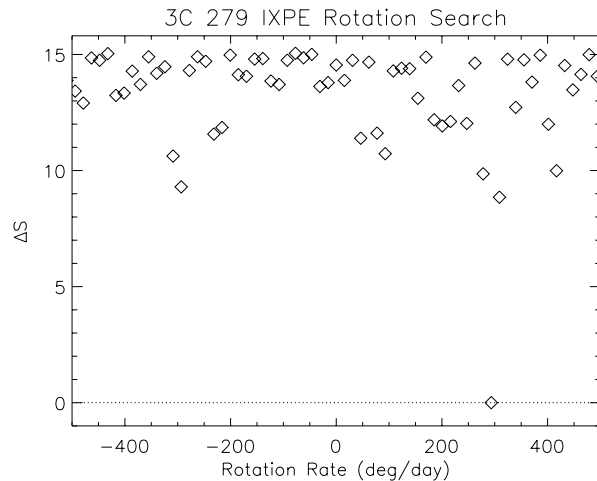


Figure 3. Example of a search for EVPA rotation, as applied to 3C 279. This source provided the largest log-likelihood difference of this group of blazars. A value of ΔS as large as 15.05 is significant at the 99.95% confidence level but there were about 130 trial rates tested, giving a chance detection of a rotation of this significant of 6.8%. See Di Gesu et al. (2023) for details of how the test was conducted.

3.1. 3C 273

3C273 ($z = 0.158339$) is one of the brightest X-ray emitting LSP blazars. It is a flat spectrum radio loud quasar with a strong “Big Blue Bump” that is interpreted as optical emission from an accretion disk (Shields 1978; Malkan 1983). Consistent with the interpretation that the optical light is of thermal origin, it is notoriously unpolarized (Stockman et al. 1984; Fernandes et al. 2020; Blinov et al. 2021a); hence it is not surprising that the polarization in the BVRI bands was $< 0.5\%$ during our contemporaneous optical/infrared campaign. Complicating the interpretation of our results is that the X-ray emission in 3C 273 is most likely a mix of hot corona and jet emission (Grandi & Palumbo 2004; Chidiac et al. 2016). The non-detection ($< 9\%$) of X-ray polarization prevents us from discerning between these two possible origins of the X-ray emission.

3.2. 3C 279

3C 279 ($z = 0.538$) is one of the most rapidly varying blazars, showing minute-timescale variability in γ -rays (Ackermann et al. 2016). It is also known to show large optical EVPA variations (Kiehlmann et al. 2016) that might also be connected to repeating patterns of γ -ray activity (Blinov et al. 2021b). During the IXPE observation the source polarization was about 4% in millimeter(mm)-radio and 12% (within uncertainties) in optical/IR (BVRIR). The EVPA showed a mild decrease from $\sim 175^\circ$ to $\sim 165^\circ$ in the optical-IR bands. In a hadronic scenario, X-ray polarization should be stable – less variable than the optical polarization (Zhang et al. 2016). Given the low-amplitude, slow EVPA variability in optical, and the fact we do not find evidence for significant variations of the X-ray EVPA (see Fig. 3), we can exclude temporal depolarization effects. Thus, the fact that the optical/IR polarization degree is

Table 2. Summary of Spectropolarimetric Results

Source	N_H (10^{20} cm^{-2})	Γ	K ($10^{-3} \text{ ph cm}^{-2} \text{ s}^{-2} \text{ keV}^{-1}$)	Π_X^a
3C 273	1.68	1.80 ± 0.02	12.1	$< 12.8\%$
3C 279	2.25	1.79 ± 0.04	2.28	$< 15.5\%$
3C 454.3	6.81	1.71 ± 0.08	1.22	$< 40.3\%$
S5 0716+714	2.88	2.29 ± 0.20	0.72	$< 41.8\%$

^aThe 99% confidence upper limits on Π_X are computed using the Q and U best-fit Gaussian 1σ errors and the best fit Q/I and U/I values. See Sec. 2.2 for details.

comparable to the X-ray upper limit ($< 12.7\%$) strongly disfavors models predicting higher X-ray polarization than the optical, such as for Mrk 421 (Di Gesu et al. 2022a, 2023) and Mrk 501 (Liodakis et al. 2022).

3.3. 3C 454.3

3C 454.3 ($z = 0.859$) has had several well-studied outbursts observed across a wide swath of the electromagnetic spectrum (e.g., Jorstad et al. 2010, 2013; Weaver et al. 2019; Liodakis et al. 2020) and showed peculiar jet behavior (e.g., Traianou et al. 2022). It showed large variation in the value of Π_{O} that can reach as high as 30% (Liodakis et al. 2020). During the IXPE observation the source was at best weakly polarized. In mm-radio, we obtained only upper limits of $< 0.8\%$ at 3mm and $< 3.3\%$ at 1.3mm. The optical (VRI) polarization is below 1% with a stable EVPA within uncertainties. The unpolarized state in the optical in combination with the X-ray upper limit ($< 28\%$) prevents us from coming to any conclusion regarding the emission processes in this source but it may be interesting to re-observe this target when Π_{O} is much higher.

3.4. S5 0716+714

S5 0716+714 ($z = 0.3$) is a highly variable source that often shows intra-night variability (e.g., Gupta et al. 2012), large outbursts across the electromagnetic spectrum and TeV emission (e.g., MAGIC Collaboration et al. 2018). During the IXPE observation, the source was observed in several optical and infrared bands (BVRIJHK) showing highly variable Π_{O} between 1-13%. There is a large change in the optical EVPA before the IXPE observations (from $\sim 125^\circ$ to $\sim 50^\circ$). During the observation we observe a slow optical EVPA increase from $\sim 50^\circ$ to $\sim 100^\circ$. Unfortunately the source was in a quiescent X-ray flux state, providing an upper limit to the X-ray polarization of $< 26\%$. Given the level of optical/IR polarization, we can only exclude models that predict several factors higher X-ray polarization

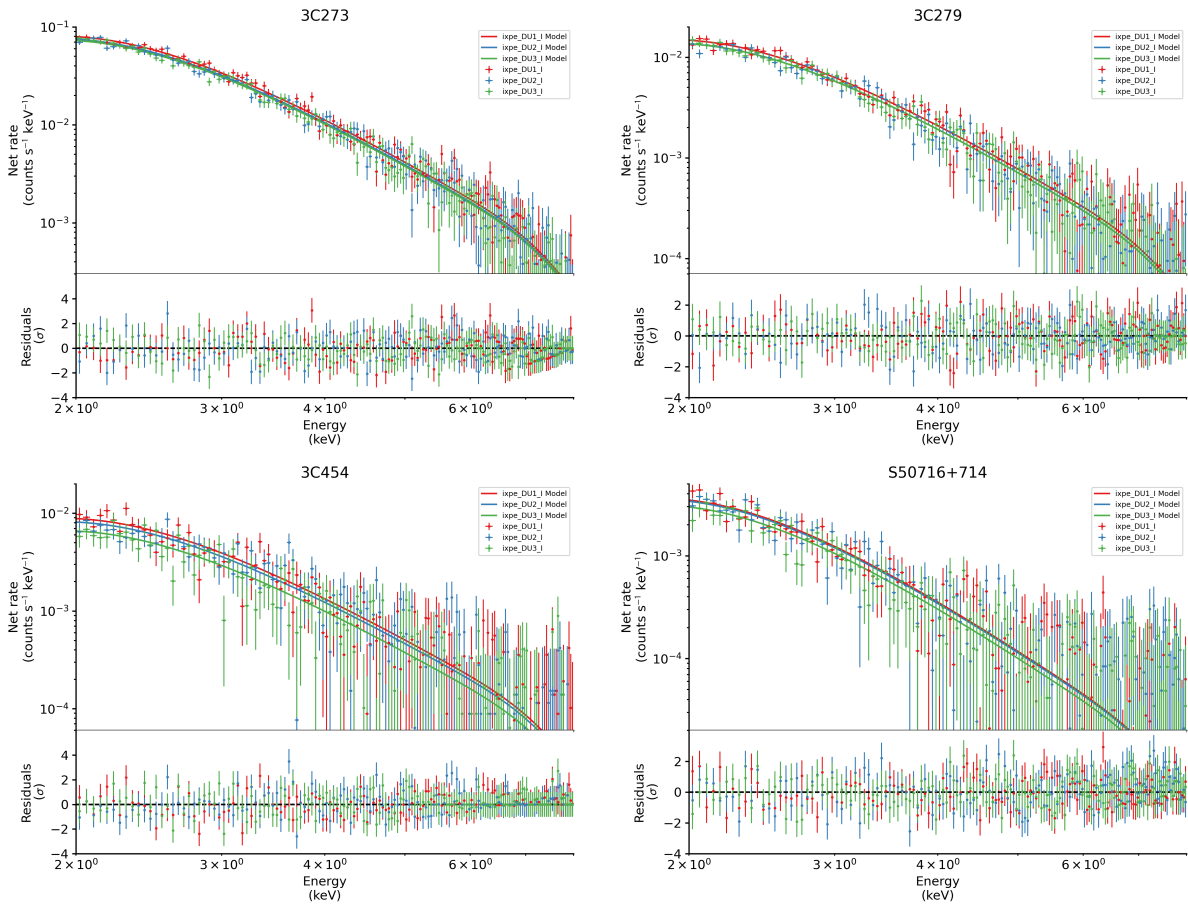


Figure 4. Background-subtracted Stokes I spectra for the four sources (from top-left to bottom-right: 3C 273, 3C 279, 3C 454.3, and S5 0716+714). In each plot, the solid lines show the best fit model (absorbed power law), and the bottom panels illustrate the residuals of the data compared to the best fit model.

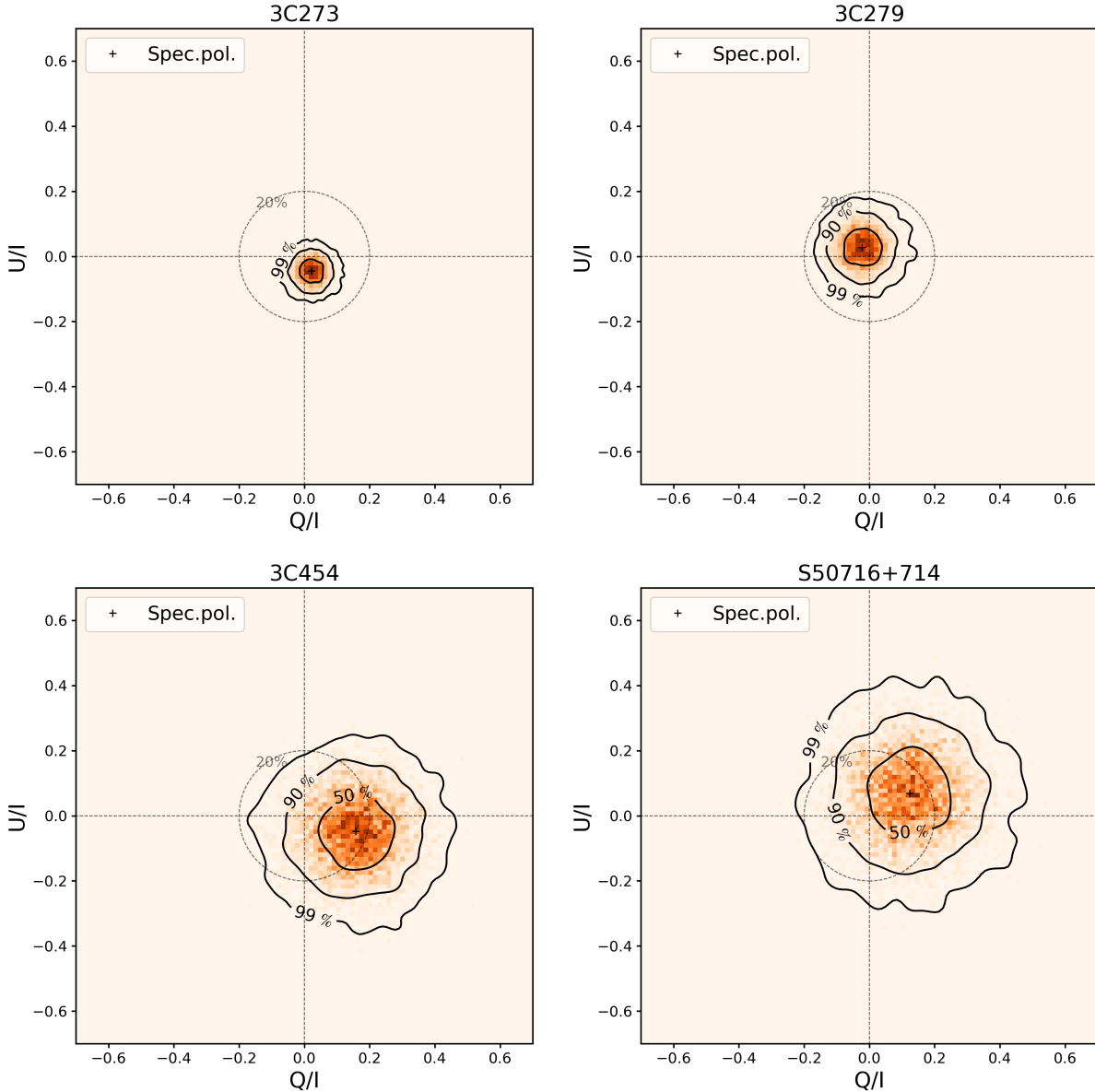


Figure 5. Stokes Q/I and U/I contour plots resulting from the spectropolarimetric fit for the four sources (from top-left to bottom-right: 3C 273, 3C 279, 3C 454.3, and S5 0716+714). Confidence levels of 50%, 90%, and 99% are shown and the dotted circles indicate the locus where the polarization fraction is 20%.

than optical. We note that the X-ray spectral index is steeper for this source than the others presented here, perhaps an indication of its ISP nature that might provide a more significant X-ray polarization detection during a soft X-ray flare.

4. SUMMARY

We presented results from the first year observations of LSP and ISP sources by IXPE, namely 3C 273, 3C 279, 3C 454.3, and S5 0716+714. All the IXPE observations were supplemented with a contemporaneous radio/optical/IR polarization campaign. None of the sources yielded a significant ($> 3\sigma$) X-ray polarization detection. Instead, we are able to constrain Π_X in the 2–8 keV band to be $< 13\%$ for 3C 273 and 3C 279 and $< 28\%$ for 3C 454.3 and S5 0716+714. The non-detection of X-ray polarization in these sources is consistent with previous IXPE results on BL Lac in both LSP and ISP states (Middei et al. 2023; Peirson et al. 2023) as well as other radio galaxies (Ehlert et al. 2022).

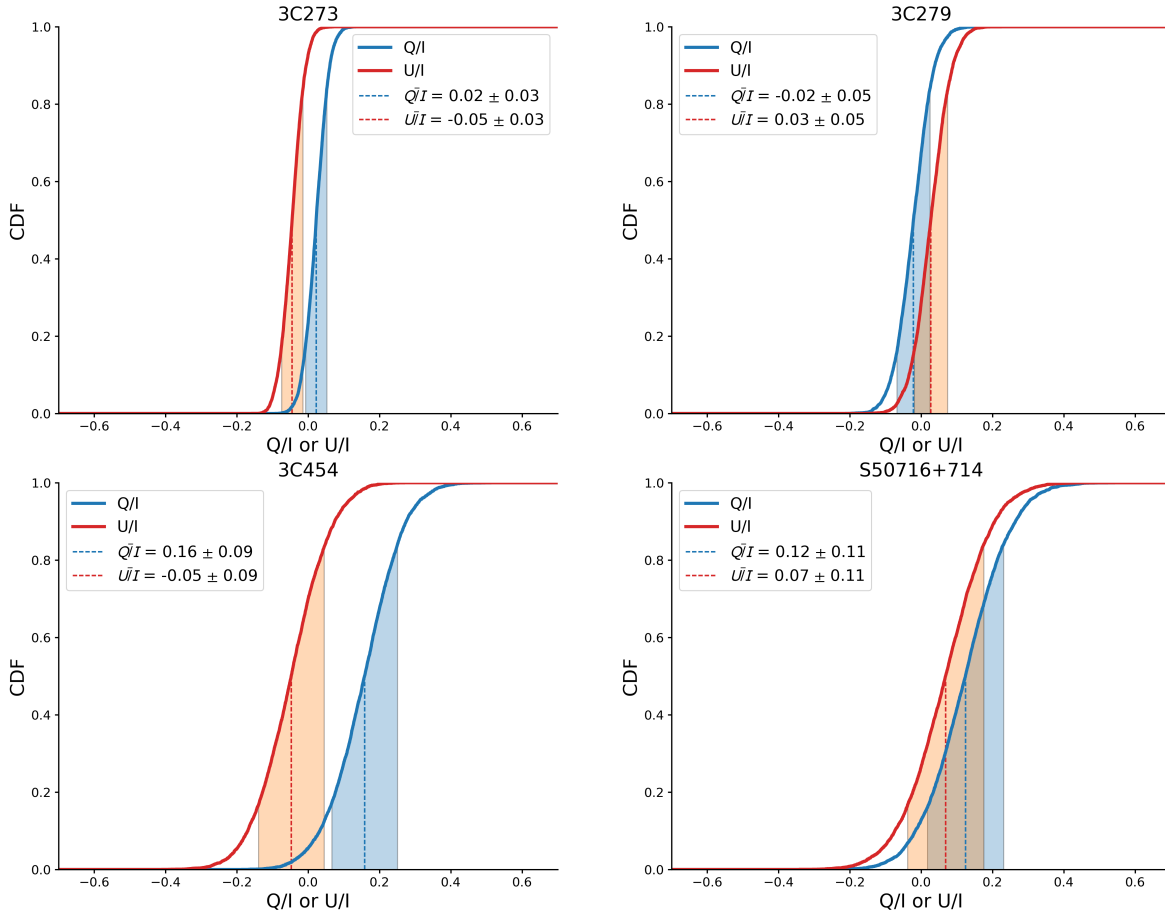


Figure 6. Stokes-Q and -U cumulative distribution functions (CDFs) for the best fit distributions for the four sources (from top-left to bottom-right: 3C 273, 3C 279, 3C 454.3, and S50716+714).

For 3C 273 and 3C 454.3, the undetected X-ray polarization could point towards inverse-Compton scattering, either external Compton or SSC, however the unpolarized optical/IR emission during the IXPE observations is preventing us from coming to definitive conclusions. For S5 0716+714, the highly variable optical polarization degree and the high upper limit ($< 26\%$) on the X-ray polarization makes any interpretation difficult. Our results disfavor a scenario where the X-ray polarization is a factor of several higher than the optical. Such a scenario can involve, for example, a pure proton synchrotron model (Zhang & Böttcher 2013; Paliya et al. 2018; Zhang et al. 2019) or scattering from relativistically moving plasma containing relatively cold electrons (Begelman & Sikora 1987).

On the other hand, 3C 279 shows fairly stable Π and EVPA in the optical/IR that remains persistently high ($> 10\%$) and the upper limit to the Π_X that is comparable ($< 12.7\%$). IXPE observations of BL Lac showed a similar picture, i.e., undetected X-ray polarization ($< 16\%$) with Π_O that is comparable or exceeds the X-ray limits (Middei et al. 2023; Peirson et al. 2023). However, in the case of BL Lac the highly variable EVPA we observe in the optical could lead to depolarization of the otherwise highly polarized proton synchrotron emission making it consistent with the Π_X limits. In the case of 3C 279 we can exclude any such depolarization effects, therefore our results strongly disfavor a significant contribution from proton synchrotron to the emission. While our results cannot yet differentiate between scattering or other hadronic processes, the emerging pattern of IXPE LSP/ISP observations suggests that $\Pi_X \lesssim 10\%$ and less than or comparable to the contemporaneous Π_O . Further IXPE observations can help further elucidate the X-ray emission mechanism in LSP/ISP blazars.

The Imaging X-ray Polarimetry Explorer (IXPE) is a joint US and Italian mission. The US contribution is supported by the National Aeronautics and Space Administration (NASA) and led and managed by its Marshall Space Flight Center (MSFC), with industry partner Ball Aerospace (contract NNM15AA18C). The Italian contribution is supported by the Italian Space Agency (Agenzia Spaziale Italiana, ASI) through contract ASI-OHBI-2017-12-I.0, agreements ASI-INAF-2017-12-H0 and ASI-INFN-2017.13-H0, and its Space Science Data Center (SSDC) with agreements ASI-INAF-2022-14-HH.0 and ASI-INFN 2021-43-HH.0, and by the Istituto Nazionale di Astrofisica (INAF) and the Istituto Nazionale di Fisica Nucleare (INFN) in Italy. This research used data products provided by the IXPE Team (MSFC, SSCD, INAF, and INFN) and distributed with additional software tools by the High-Energy Astrophysics Science Archive Research Center (HEASARC), at NASA Goddard Space Flight Center (GSFC). Funding for this work was provided in part by contract 80MSFC17C0012 from the MSFC to MIT in support of the IXPE project. Support for this work was provided in part by the National Aeronautics and Space Administration (NASA) through the Smithsonian Astrophysical Observatory (SAO) contract SV3-73016 to MIT for support of the Chandra X-Ray Center (CXC), which is operated by SAO for and on behalf of NASA under contract NAS8-03060. This research has made use of data from the RoboPol programme, a collaboration between Caltech, the University of Crete, IA-FORTH, IUCAA, the MPIfR, and the Nicolaus Copernicus University, which was conducted at Skinakas Observatory in Crete, Greece. The IAA-CSIC co-authors acknowledge financial support from the Spanish "Ministerio de Ciencia e Innovacion" (MCINN) through the "Center of Excellence Severo Ochoa" award for the Instituto de Astrofísica de Andalucía-CSIC (SEV-2017-0709). Acquisition and reduction of the POLAMI, TOP-MAPCAR, and OSN data was supported in part by MICINN through grants AYA2016-80889-P and PID2019-107847RB-C44. Some of the data are based on observations collected at the Observatorio de Sierra Nevada, owned and operated by the Instituto de Astrofísica de Andalucía (IAA-CSIC). Further data are based on observations collected at the Centro Astronómico Hispano-Alemán (CAHA), operated jointly by Junta de Andalucía and Consejo Superior de Investigaciones Científicas (IAA-CSIC). The POLAMI observations were carried out at the IRAM 30m Telescope. IRAM is supported by INSU/CNRS (France), MPG (Germany) and IGN (Spain). Some of the data reported here are based on observations obtained at the Hale Telescope, Palomar Observatory as part of a continuing collaboration between the California Institute of Technology, NASA/JPL, Yale University, and the National Astronomical Observatories of China. GVP acknowledges support by NASA through the NASA Hubble Fellowship grant #HST-HF2-51444.001-A awarded by the Space Telescope Science Institute, which is operated by the Association of Universities for Research in Astronomy, Inc., under NASA contract NAS5-26555. The data in this study include observations made with the Nordic Optical Telescope, owned in collaboration by the University of Turku and Aarhus University, and operated jointly by Aarhus University, the University of Turku and the University of Oslo, representing Denmark, Finland and Norway, the University of Iceland and Stockholm University at the Observatorio del Roque de los Muchachos, La Palma, Spain, of the Instituto de Astrofísica de Canarias. The data presented here were obtained in part with ALFOSC, which is provided by the Instituto de Astrofísica de Andalucía (IAA) under a joint agreement with the University of Copenhagen and NOT. E. L. was supported by Academy of Finland projects 317636 and 320045. D.B., S.K., R.S., N. M., acknowledge support from the European Research Council (ERC) under the European Unions Horizon 2020 research and innovation programme under grant agreement No. 771282. CC acknowledges support by the European Research Council (ERC) under the HORIZON ERC Grants 2021 programme under grant agreement No. 101040021. The Dipol-2 polarimeter was built in cooperation by the University of Turku, Finland, and the Leibniz Institut für Sonnenphysik, Germany, with support from the Leibniz Association grant SAW-2011-KIS-7. This work was supported by JST, the establishment of university fellowships towards the creation of science technology innovation, Grant Number JPMJFS2129. This work was supported by Japan Society for the Promotion of Science (JSPS) KAKENHI Grant Numbers JP21H01137. This work was also partially supported by Optical and Near-Infrared Astronomy Inter-University Cooperation Program from the Ministry of Education, Culture, Sports, Science and Technology (MEXT) of Japan. We are grateful to the observation and operating members of Kanata Telescope. The research at Boston University was supported in part by National Science Foundation grant AST-2108622, NASA Fermi Guest Investigator grant 80NSSC22K1571, and NASA Swift Guest Investigator grant 80NSSC22K0537. This study used observations conducted with the 1.8 m Perkins Telescope Observatory (PTO) in Arizona (USA), which is owned and operated by Boston University.

Facilities: AZT-8, Calar Alto, IRAM-30m, IXPE, LX-200, Kanata, Nordic Optical Telescope, Palomar, Perkins, Skinakas Observatory, Swift, T60, T90, T150

Software: `ixpeobssim` (Baldini et al. 2022), `Astropy` (Astropy Collaboration et al. 2013, 2018), `Photutils` (Bradley et al. 2019), `NumPy` and `SciPy` (Virtanen et al. 2020), `IPython` (Perez & Granger 2007), `HEASoft 6.30.1`³ (NASA High Energy Astrophysics Science Archive Research Center (HEASARC) 2014), `3ML` (Vianello et al. 2015)

REFERENCES

- Abdo, A. A., Ackermann, M., Agudo, I., et al. 2010, *ApJ*, 716, 30, doi: [10.1088/0004-637X/716/1/30](https://doi.org/10.1088/0004-637X/716/1/30)
- Ackermann, M., Anantua, R., Asano, K., et al. 2016, *ApJL*, 824, L20, doi: [10.3847/2041-8205/824/2/L20](https://doi.org/10.3847/2041-8205/824/2/L20)
- Agudo, I., Thum, C., Ramakrishnan, V., et al. 2018a, *MNRAS*, 473, 1850, doi: [10.1093/mnras/stx2437](https://doi.org/10.1093/mnras/stx2437)
- Agudo, I., Thum, C., Molina, S. N., et al. 2018b, *MNRAS*, 474, 1427, doi: [10.1093/mnras/stx2435](https://doi.org/10.1093/mnras/stx2435)
- Akitaya, H., Moritani, Y., Ui, T., et al. 2014, in *Society of Photo-Optical Instrumentation Engineers (SPIE) Conference Series*, Vol. 9147, *Ground-based and Airborne Instrumentation for Astronomy V*, ed. S. K. Ramsay, I. S. McLean, & H. Takami, 91474O, doi: [10.1117/12.2054577](https://doi.org/10.1117/12.2054577)
- Astropy Collaboration, Robitaille, T. P., Tollerud, E. J., et al. 2013, *A&A*, 558, A33, doi: [10.1051/0004-6361/201322068](https://doi.org/10.1051/0004-6361/201322068)
- Astropy Collaboration, Price-Whelan, A. M., Sipőcz, B. M., et al. 2018, *AJ*, 156, 123, doi: [10.3847/1538-3881/aabc4f](https://doi.org/10.3847/1538-3881/aabc4f)
- Baldini, L., Bucciantini, N., Lalla, N. D., et al. 2022, *SoftwareX*, 19, 101194, doi: [10.1016/j.softx.2022.101194](https://doi.org/10.1016/j.softx.2022.101194)
- Begelman, M. C., & Sikora, M. 1987, *ApJ*, 322, 650, doi: [10.1086/165760](https://doi.org/10.1086/165760)
- Berdyugin, A., Piirola, V., & Poutanen, J. 2019, in *Astrophysics and Space Science Library*, Vol. 460, *Astronomical Polarisation from the Infrared to Gamma Rays*, ed. R. Mignani, A. Shearer, A. Słowikowska, & S. Zane, 33, doi: [10.1007/978-3-030-19715-5_3](https://doi.org/10.1007/978-3-030-19715-5_3)
- Berdyugin, A. V., Berdyugina, S. V., & Piirola, V. 2018, in *Society of Photo-Optical Instrumentation Engineers (SPIE) Conference Series*, Vol. 10702, *Ground-based and Airborne Instrumentation for Astronomy VII*, ed. C. J. Evans, L. Simard, & H. Takami, 107024Z, doi: [10.1117/12.2312695](https://doi.org/10.1117/12.2312695)
- Blandford, R., Meier, D., & Readhead, A. 2019, *ARA&A*, 57, 467, doi: [10.1146/annurev-astro-081817-051948](https://doi.org/10.1146/annurev-astro-081817-051948)
- Blinov, D., Kiehlmann, S., Pavlidou, V., et al. 2021a, *MNRAS*, 501, 3715, doi: [10.1093/mnras/staa3777](https://doi.org/10.1093/mnras/staa3777)
- Blinov, D., Jorstad, S. G., Larionov, V. M., et al. 2021b, *MNRAS*, 505, 4616, doi: [10.1093/mnras/stab1484](https://doi.org/10.1093/mnras/stab1484)
- Bradley, L., Sipőcz, B., Robitaille, T., et al. 2019, `astropy/photutils: v0.7.2, v0.7.2`, Zenodo, Zenodo, doi: [10.5281/zenodo.3568287](https://doi.org/10.5281/zenodo.3568287)
- Chidiac, C., Rani, B., Krichbaum, T. P., et al. 2016, *A&A*, 590, A61, doi: [10.1051/0004-6361/201628347](https://doi.org/10.1051/0004-6361/201628347)
- Clemens, D. P., Pinnick, A. F., & Pavel, M. D. 2012, *ApJS*, 200, 20, doi: [10.1088/0067-0049/200/2/20](https://doi.org/10.1088/0067-0049/200/2/20)
- Di Gesu, L., Tavecchio, F., Donnarumma, I., et al. 2022a, *A&A*, 662, A83, doi: [10.1051/0004-6361/202243168](https://doi.org/10.1051/0004-6361/202243168)
- Di Gesu, L., Donnarumma, I., Tavecchio, F., et al. 2022b, *ApJL*, 938, L7, doi: [10.3847/2041-8213/ac913a](https://doi.org/10.3847/2041-8213/ac913a)
- Di Gesu, L., Marshall, H. L., Ehlert, S. R., et al. 2023, *Nature Astronomy*, doi: [10.1038/s41550-023-02032-7](https://doi.org/10.1038/s41550-023-02032-7)
- Ehlert, S. R., Ferrazzoli, R., Marinucci, A., et al. 2022, *ApJ*, 935, 116, doi: [10.3847/1538-4357/ac8056](https://doi.org/10.3847/1538-4357/ac8056)
- Fernandes, S., Patiño-Álvarez, V. M., Chavushyan, V., Schlegel, E. M., & Valdés, J. R. 2020, *MNRAS*, 497, 2066, doi: [10.1093/mnras/staa2013](https://doi.org/10.1093/mnras/staa2013)
- Grandi, P., & Palumbo, G. G. C. 2004, *Science*, 306, 998, doi: [10.1126/science.1101787](https://doi.org/10.1126/science.1101787)
- Gupta, A. C., Krichbaum, T. P., Wiita, P. J., et al. 2012, *MNRAS*, 425, 1357, doi: [10.1111/j.1365-2966.2012.21550.x](https://doi.org/10.1111/j.1365-2966.2012.21550.x)
- Hovatta, T., Lindfors, E., Blinov, D., et al. 2016, *A&A*, 596, A78, doi: [10.1051/0004-6361/201628974](https://doi.org/10.1051/0004-6361/201628974)
- Hughes, P. A., Aller, H. D., & Aller, M. F. 1985, *ApJ*, 298, 301, doi: [10.1086/163611](https://doi.org/10.1086/163611)
- Jorstad, S. G., Marscher, A. P., Larionov, V. M., et al. 2010, *ApJ*, 715, 362, doi: [10.1088/0004-637X/715/1/362](https://doi.org/10.1088/0004-637X/715/1/362)
- Jorstad, S. G., Marscher, A. P., Smith, P. S., et al. 2013, *ApJ*, 773, 147, doi: [10.1088/0004-637X/773/2/147](https://doi.org/10.1088/0004-637X/773/2/147)
- Kawabata, K. S., Okazaki, A., Akitaya, H., et al. 1999, *PASP*, 111, 898, doi: [10.1086/316387](https://doi.org/10.1086/316387)
- Kiehlmann, S., Savolainen, T., Jorstad, S. G., et al. 2016, *A&A*, 592, C1, doi: [10.1051/0004-6361/201527725e](https://doi.org/10.1051/0004-6361/201527725e)
- Kosenkov, I. A., Berdyugin, A. V., Piirola, V., et al. 2017, *MNRAS*, 468, 4362, doi: [10.1093/mnras/stx779](https://doi.org/10.1093/mnras/stx779)
- Krawczynski, H. 2012, *ApJ*, 744, 30, doi: [10.1088/0004-637X/744/1/30](https://doi.org/10.1088/0004-637X/744/1/30)
- Liodakis, I., Peirson, A. L., & Romani, R. W. 2019, *ApJ*, 880, 29, doi: [10.3847/1538-4357/ab2719](https://doi.org/10.3847/1538-4357/ab2719)
- Liodakis, I., Blinov, D., Jorstad, S. G., et al. 2020, *ApJ*, 902, 61, doi: [10.3847/1538-4357/abb1b8](https://doi.org/10.3847/1538-4357/abb1b8)

³ <http://heasarc.gsfc.nasa.gov/ftools>

- Lioudakis, I., Marscher, A. P., Agudo, I., et al. 2022, *Nature*, 611, 677, doi: [10.1038/s41586-022-05338-0](https://doi.org/10.1038/s41586-022-05338-0)
- Lyutikov, M., Pariev, V. I., & Gabuzda, D. C. 2005, *MNRAS*, 360, 869, doi: [10.1111/j.1365-2966.2005.08954.x](https://doi.org/10.1111/j.1365-2966.2005.08954.x)
- MAGIC Collaboration, Ahnen, M. L., Ansoldi, S., et al. 2018, *A&A*, 619, A45, doi: [10.1051/0004-6361/201832677](https://doi.org/10.1051/0004-6361/201832677)
- Malkan, M. A. 1983, *ApJ*, 268, 582, doi: [10.1086/160981](https://doi.org/10.1086/160981)
- Maraschi, L., Foschini, L., Ghisellini, G., Tavecchio, F., & Sambruna, R. M. 2008, *Monthly Notices of the Royal Astronomical Society*, 391, 1981, doi: [10.1111/j.1365-2966.2008.14030.x](https://doi.org/10.1111/j.1365-2966.2008.14030.x)
- Marscher, A. P., & Gear, W. K. 1985, *ApJ*, 298, 114, doi: [10.1086/163592](https://doi.org/10.1086/163592)
- Marscher, A. P., & Jorstad, S. G. 2022, *Universe*, 8, 644, doi: [10.3390/universe8120644](https://doi.org/10.3390/universe8120644)
- Marshall, H. L. 2021, *ApJ*, 907, 82, doi: [10.3847/1538-4357/abcfc3](https://doi.org/10.3847/1538-4357/abcfc3)
- . 2023, *ApJ*, submitted
- Masiero, J. R., Tinyanont, S., & Millar-Blanchaer, M. A. 2022, *PSJ*, 3, 90, doi: [10.3847/PSJ/ac6342](https://doi.org/10.3847/PSJ/ac6342)
- Middei, R., Perri, M., Puccetti, S., et al. 2023, *The Astrophysical Journal Letters*, 953, L28, doi: [10.3847/2041-8213/acec3e](https://doi.org/10.3847/2041-8213/acec3e)
- Middei, R., Lioudakis, I., Perri, M., et al. 2023, *ApJL*, 942, L10, doi: [10.3847/2041-8213/aca281](https://doi.org/10.3847/2041-8213/aca281)
- Millar-Blanchaer, M. A., Tinyanont, S., Jovanovic, N., et al. 2021, in *Ground-based and Airborne Instrumentation for Astronomy VIII*, ed. C. J. Evans, J. J. Bryant, & K. Motohara, Vol. 11447, *International Society for Optics and Photonics (SPIE)*, 1315 – 1332, doi: [10.1117/12.2562762](https://doi.org/10.1117/12.2562762)
- NASA High Energy Astrophysics Science Archive Research Center (HEASARC). 2014, *HEASoft: Unified Release of FTOOLS and XANADU*, *Astrophysics Source Code Library*, record ascl:1408.004. <http://ascl.net/1408.004>
- Nilsson, K., Lindfors, E., Takalo, L. O., et al. 2018, *A&A*, 620, A185, doi: [10.1051/0004-6361/201833621](https://doi.org/10.1051/0004-6361/201833621)
- Paliya, V. S., Zhang, H., Böttcher, M., et al. 2018, *ApJ*, 863, 98, doi: [10.3847/1538-4357/aad1f0](https://doi.org/10.3847/1538-4357/aad1f0)
- Panopoulou, G., Tassis, K., Blinov, D., et al. 2015, *MNRAS*, 452, 715, doi: [10.1093/mnras/stv1301](https://doi.org/10.1093/mnras/stv1301)
- Peirson, A. L., Lioudakis, I., & Romani, R. W. 2022, *ApJ*, 931, 59, doi: [10.3847/1538-4357/ac6a54](https://doi.org/10.3847/1538-4357/ac6a54)
- Peirson, A. L., Negro, M., Lioudakis, I., et al. 2023, *ApJL*, 948, L25, doi: [10.3847/2041-8213/acd242](https://doi.org/10.3847/2041-8213/acd242)
- Perez, F., & Granger, B. E. 2007, *Computing in Science and Engineering*, 9, 21, doi: [10.1109/MCSE.2007.53](https://doi.org/10.1109/MCSE.2007.53)
- Piirola, V. 1973, *A&A*, 27, 383
- Piirola, V., Kosenkov, I. A., Berdyugin, A. V., Berdyugina, S. V., & Poutanen, J. 2021, *AJ*, 161, 20, doi: [10.3847/1538-3881/abc74f](https://doi.org/10.3847/1538-3881/abc74f)
- Ramaprakash, A. N., Rajarshi, C. V., Das, H. K., et al. 2019, *MNRAS*, 485, 2355, doi: [10.1093/mnras/stz557](https://doi.org/10.1093/mnras/stz557)
- Shields, G. A. 1978, *Nature*, 272, 706, doi: [10.1038/272706a0](https://doi.org/10.1038/272706a0)
- Stockman, H. S., Moore, R. L., & Angel, J. R. P. 1984, *ApJ*, 279, 485, doi: [10.1086/161912](https://doi.org/10.1086/161912)
- Tavecchio, F., Landoni, M., Sironi, L., & Coppi, P. 2018, *MNRAS*, 480, 2872, doi: [10.1093/mnras/sty1491](https://doi.org/10.1093/mnras/sty1491)
- Thum, C., Agudo, I., Molina, S. N., et al. 2018, *MNRAS*, 473, 2506, doi: [10.1093/mnras/stx2436](https://doi.org/10.1093/mnras/stx2436)
- Tinyanont, S., Millar-Blanchaer, M. A., Nilsson, R., et al. 2019a, *PASP*, 131, 025001, doi: [10.1088/1538-3873/aaef0f](https://doi.org/10.1088/1538-3873/aaef0f)
- Tinyanont, S., Millar-Blanchaer, M., Jovanovic, N., et al. 2019b, in *Society of Photo-Optical Instrumentation Engineers (SPIE) Conference Series*, Vol. 11132, *Polarization Science and Remote Sensing IX*, 1113209, doi: [10.1117/12.2529863](https://doi.org/10.1117/12.2529863)
- Traianou, E., Krichbaum, T., Gomez, J. L., et al. 2022, in *44th COSPAR Scientific Assembly*. Held 16-24 July, Vol. 44, 2037
- Vianello, G., Lauer, R. J., Younk, P., et al. 2015, *arXiv e-prints*, arXiv:1507.08343. <https://arxiv.org/abs/1507.08343>
- Virtanen, P., Gommers, R., Oliphant, T. E., et al. 2020, *Nature Methods*, 17, 261, doi: [10.1038/s41592-019-0686-2](https://doi.org/10.1038/s41592-019-0686-2)
- Weaver, Z. R., Balonek, T. J., Jorstad, S. G., et al. 2019, *ApJ*, 875, 15, doi: [10.3847/1538-4357/ab0e7c](https://doi.org/10.3847/1538-4357/ab0e7c)
- Weisskopf, M. C., Soffitta, P., Baldini, L., et al. 2022, *Journal of Astronomical Telescopes, Instruments, and Systems*, 8, 026002, doi: [10.1117/1.JATIS.8.2.026002](https://doi.org/10.1117/1.JATIS.8.2.026002)
- Zhang, H., & Böttcher, M. 2013, *ApJ*, 774, 18, doi: [10.1088/0004-637X/774/1/18](https://doi.org/10.1088/0004-637X/774/1/18)
- Zhang, H., Diltz, C., & Böttcher, M. 2016, *ApJ*, 829, 69, doi: [10.3847/0004-637X/829/2/69](https://doi.org/10.3847/0004-637X/829/2/69)
- Zhang, H., Fang, K., Li, H., et al. 2019, *ApJ*, 876, 109, doi: [10.3847/1538-4357/ab158d](https://doi.org/10.3847/1538-4357/ab158d)

Table 3. Polarization Results Contemporaneous with the IXPE observation of 3C 273.

Telescope	Π (%)	s_{Π}	ψ (deg.)	s_{ψ}
POLAMI (3 mm)	5.55 ± 1.17	0.06	146 ± 6	0.3
POLAMI (1.3 mm)	5.23 ± 0.8	0.58	150 ± 4	6.6
AZT-8 & LX-200 (R-band)	0.38 ± 0.23	–	111 ± 14	–
NOT (B-band)	0.45 ± 0.13	0.05	60 ± 9	1.45
NOT (V-band)	0.31 ± 0.11	0.07	550 ± 11	10.5
NOT (R-band)	0.23 ± 0.1	0.05	61 ± 14	3.4
NOT (I-band)	0.18 ± 0.1	0.09	50 ± 21	11.1
Skinakas (R-band)	0.2 ± 0.1	–	47 ± 17	–

NOTE—The uncertainties for Π and ψ (i.e. EVPA) are either the uncertainty of the measurement or the median uncertainty in the case of multiple measurements. The quantities s_{Π} and s_{ψ} represent the standard deviations of Π or ψ , respectively.

Table 4. Polarization Results Contemporaneous with the IXPE observation of 3C 279.

Telescope	Π (%)	s_{Π}	ψ (deg.)	s_{ψ}
POLAMI (3 mm)	4.09 ± 0.34	0.15	359 ± 2	0.84
POLAMI (1.3 mm)	< 4.6	–	–	–
AZT-8 & LX-200 (R-band)	10.2 ± 1	0.97	169 ± 3	5.5
Calar Alto & SNO (R-band)	11 ± 2	3.4	154 ± 6	10.6
Kanata (R-band)	11.75 ± 0.42	–	163 ± 1	–
Kanata (J-band)	8.88 ± 0.75	–	166 ± 3	–
NOT (B-band)	10.77 ± 0.35	0.03	169 ± 1	2.26
NOT (V-band)	10.86 ± 0.26	0.23	167 ± 0.7	1.1
NOT (R-band)	11.01 ± 0.26	0.01	164.4 ± 0.6	2.04
NOT (I-band)	10.79 ± 0.36	0.07	163.3 ± 1	1.72
Perkins (H-band)	11.54 ± 0.5	1.13	175 ± 1	4.06
Skinakas (R-band)	11.55 ± 0.33	–	160.4 ± 0.8	–

NOTE—See the Table 3 note.

APPENDIX

A. MULTIWAVELENGTH POLARIZATION OBSERVATIONS

Contemporaneous to the IXPE observations several telescopes across the world provided multiwavelength polarization observations from radio to optical. In the mm–radio spectral bands, all the sources were observed with the IRAM-30m telescope as part of the Polarimetric Monitoring of AGN at Millimeter Wavelengths (POLAMI⁴) project at 3.5 mm (86.24 GHz) and 1.3 mm (228.93 GHz) (Agudo et al. 2018b,a; Thum et al. 2018). S5 0716+714, 3C 273, and 3C 279 were observed in the J, H, and K infrared bands with using the 200-inch Palomar Hale telescope and the WIRC+Pol⁵ instrument (Tinyanont et al. 2019a,b; Millar-Blanchaer et al. 2021; Masiero et al. 2022); the Kanata telescope using the Hiroshima Optical and Near-InfraRed camera (HONIR, Kawabata et al. 1999; Akitaya et al. 2014); and the IR camera MIMIR⁶ (Clemens et al. 2012) at the Perkins Telescope (PTO, Flagstaff, AZ). In the optical, all the sources we observed in B, V, R, I bands by the AZT-8 & LX-200 telescopes (St. Petersburg University); Calar Alto and Sierra Nevada observatories; DIPOL-2 polarimeter at the Haleakala observatory T60 telescope (Piirola 1973; Kosenkov et al. 2017; Berdyugin et al. 2018, 2019; Piirola et al. 2021); HONIR at the Kanata telescope; Alhambra Faint Object Spectrograph and Camera (ALFOSC) at the Nordic Optical Telescope (Hovatta et al. 2016; Nilsson et al.

⁴ <http://polami.iaa.es/>

⁵ https://github.com/WIRC-Pol/wirc_drp

⁶ <https://people.bu.edu/clemens/mimir/index.html>

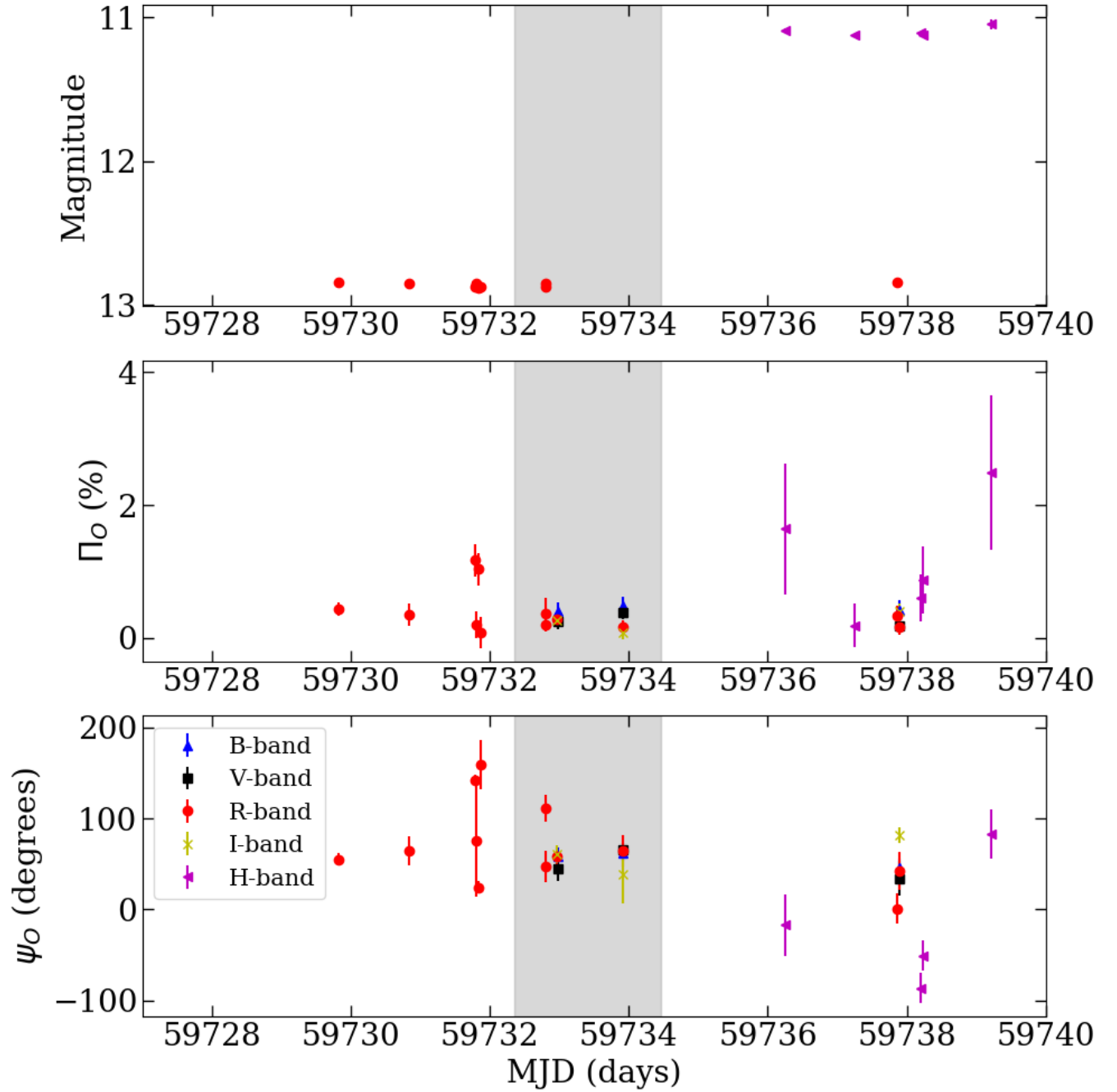


Figure 7. Contemporaneous optical and infrared observations of 3C 273. The top panel shows the brightness in magnitudes, middle panel the polarization degree, and bottom panel the EVPA. The grey shaded area marks the duration of the IXPE observation.

2018), and the RoboPol polarimeters at the Skinakas observatory (Panopoulou et al. 2015; Ramaprakash et al. 2019; Blinov et al. 2021a). Figures 7, 8, 9, and 10 show the observations for the individual sources and Tables 3, 4, 5, and 6 the median values for the polarization degree and EVPA during the IXPE observations.

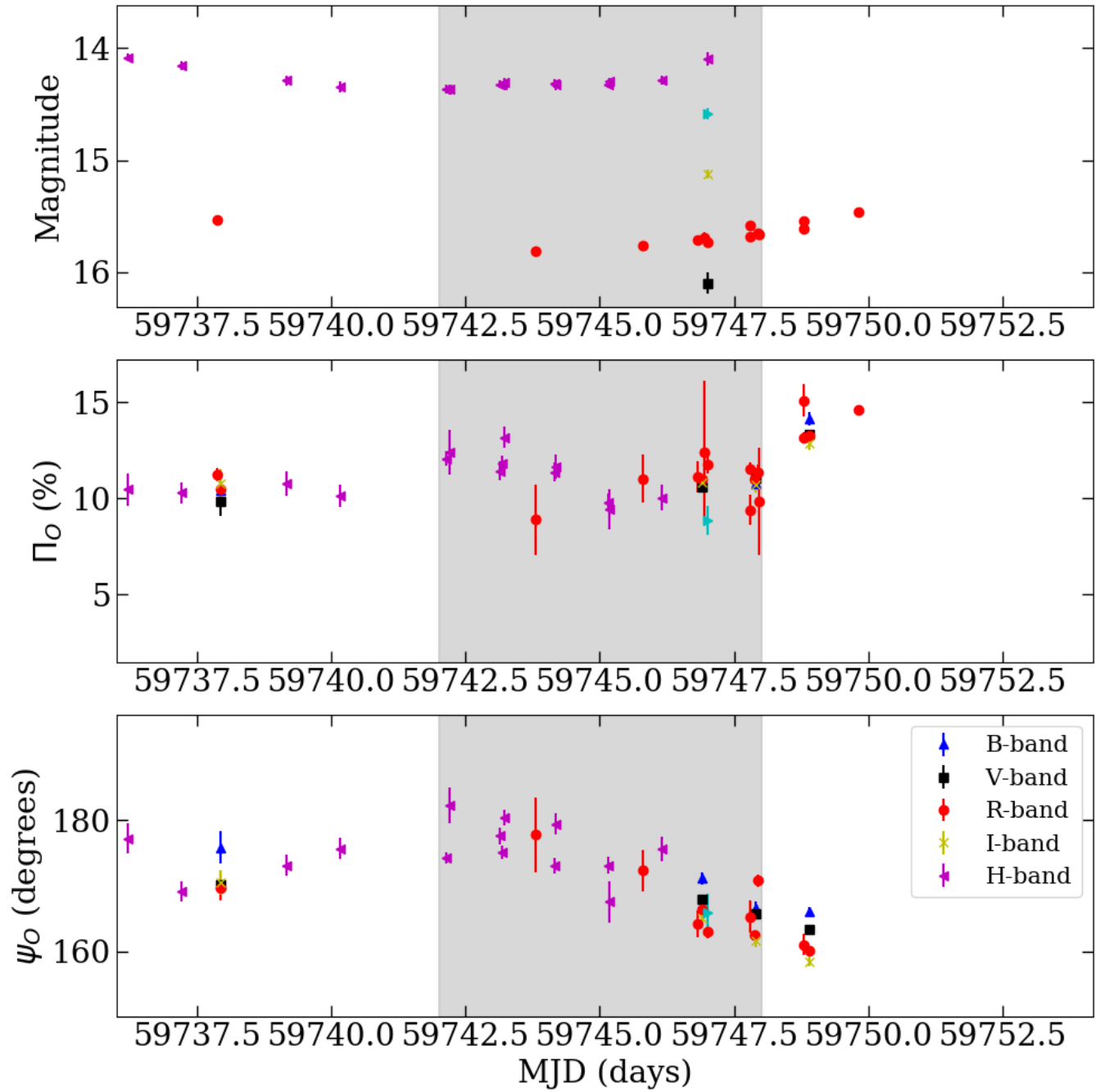


Figure 8. Same as Fig. 7 but for 3C 279.

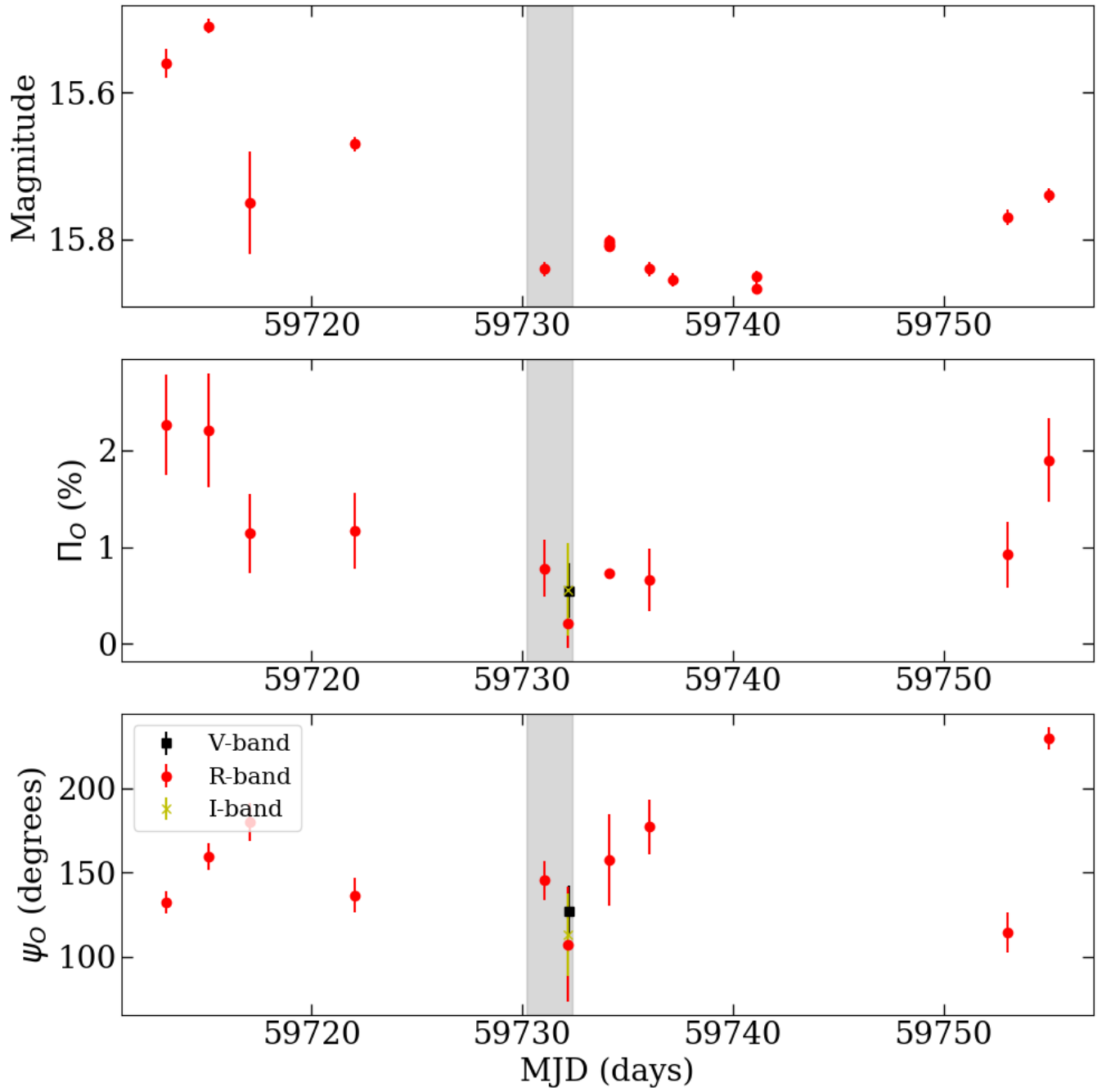


Figure 9. Same as Fig. 7 but for 3C 454.3.

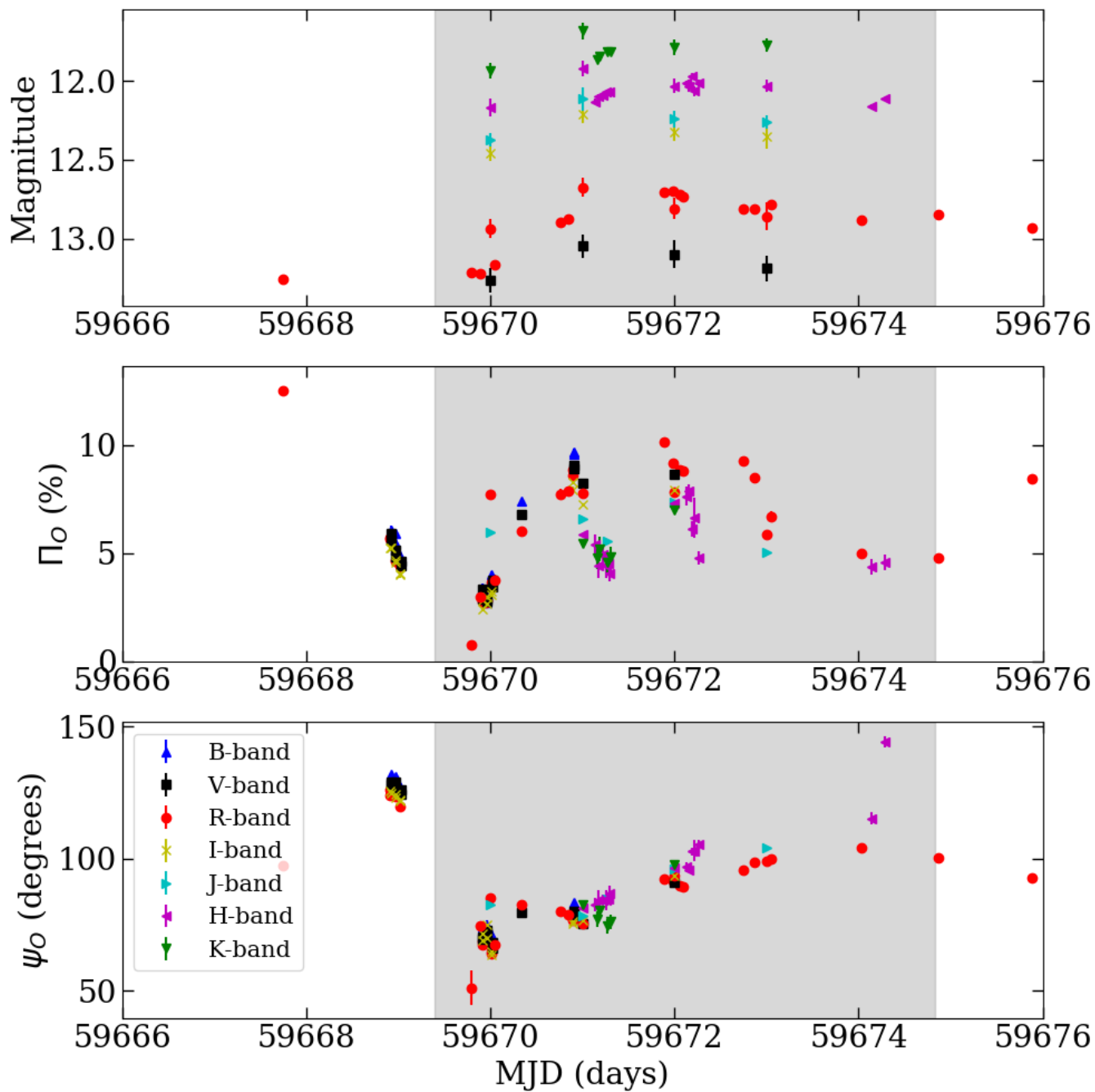


Figure 10. Same as Fig. 7 but for S5 0716+714.

Table 5. Polarization Results Contemporaneous with the IXPE observation of 3C 454.3.

Telescope	Π (%)	s_{Π}	ψ (deg.)	s_{ψ}
POLAMI (3 mm)	< 0.82	–	–	–
POLAMI (1.3 mm)	< 3.3	–	–	–
AZT-8 & LX-200 (R-band)	< 1	–	–	–
Calar Alto (R-band)	0.72 ± 0.3	0.28	157 ± 15	27
NOT (B-band)	< 1	–	–	–
NOT (V-band)	0.55 ± 0.3	–	127 ± 15	–
NOT (R-band)	0.21 ± 0.25	–	107 ± 34	–
NOT (I-band)	0.56 ± 0.48	–	113 ± 25	–
Skinakas (R-band)	0.67 ± 0.33	–	145 ± 12	–

NOTE—See the Table 3 note.

Table 6. Polarization Results Contemporaneous with the IXPE observation of S5 0716+714.

Telescope	Π (%)	s_{Π}	ψ (deg.)	s_{ψ}
POLAMI (3 mm)	< 1.1	–	–	–
POLAMI (1.3 mm)	< 3.8	–	–	–
AZT-8 & LX-200 (R-band)	7.86 ± 0.17	2.76	89.7 ± 0.6	14.24
Kanata (R-band)	7.75 ± 0.04	0.83	89.2 ± 0.13	9.01
Kanata (J-band)	6.28 ± 0.06	0.84	89.4 ± 0.2	10.24
NOT (B-band)	3.59 ± 0.18	2.74	74 ± 1.4	5.05
NOT (V-band)	3.39 ± 0.14	2.53	71.2 ± 1.3	4.54
NOT (R-band)	3.19 ± 0.14	2.47	69 ± 1.2	4.57
NOT (I-band)	3.03 ± 0.13	2.28	71 ± 1.2	4.41
Palomar (J-band)	4.52 ± 0.07	–	85 ± 1	–
Palomar (H-band)	5.57 ± 0.07	0	85 ± 1	–
Perkins (H-band)	4.86 ± 0.38	1.26	96 ± 2.2	16.95
Perkins (K-band)	4.81 ± 0.49	0.22	77 ± 2.9	2.25
T60 (B-band)	7.41 ± 0.12	–	82.1 ± 0.5	–
T60 (V-band)	6.8 ± 0.16	–	79.8 ± 0.7	–
T60 (R-band)	6.04 ± 0.15	–	82.8 ± 0.7	–

NOTE—See the Table 3 note.